

A TECHNIQUE TO ASSESS WIND UPLIFT PERFORMANCE OF STANDING SEAM METAL ROOFS

DAVID O. PREVATT, SCOTT D. SCHIFF and PETER R. SPARKS

Department of Civil Engineering
Clemson University
Clemson, S.C.

Performance and test criteria were evaluated for standing seam metal roofs subjected to wind uplift pressure. Influence surfaces for uplift load on the fasteners attaching the roof clips to the purlins were determined for roof specimens at various base pressures. The influence surfaces were found to change as the static base pressure was increased, reflecting changes in the load transfer mechanisms. Reasons are presented to explain how the structural properties of the roof changed as the uplift loads were increased.

An equivalent uniform-pressure load time-history for an interior roof clip fastener was developed by personnel at the University of Western Ontario by combining the influence surfaces with wind tunnel data and a Hurricane Andrew simulation. By using the BRERWULF test set-up to produce this dynamic trace on a 12 ft. x 26 ft. (3.66 m x 7.92 m) roof specimen, the roof performance and load distribution among fasteners were observed. Those data were compared with similar results obtained during a series of static pressure tests, as specified in ASTM E 1592-94.

It was found from these studies that the non-linear structural response and large displacements of standing seam roofs under upward pressures cause variations in load distribution among roof clips, which cannot be easily determined from simple tributary area assumptions. Thus, the failure loads of clips are difficult to predict from static pressure measurements alone.

The pros and cons of dynamic test programs are discussed and recommendations are made for improving current static test procedures, which might lead to more realistic test methods for standing seam metal roof systems.

KEYWORDS

Clip load, influence surfaces, standing seam metal roof, static air pressure and wind uplift performance.

INTRODUCTION

Full-scale measurements from the Texas Tech building,¹ as well as wind tunnel studies,² have shown that pressure variations on a roof due to the wind are highly variable, both spatially and in time. The pressures created by the wind are highly fluctuating, partly as a result of the gustiness of the wind, but also because of local vortex shedding from the edges of the structure itself. The pressures are also not uniformly distributed over the surface of the structure, but vary with position, making the determination of critical

load effects on roofing components somewhat difficult.

Past investigations have indicated the variable performance of standing seam metal roofs during windstorms.³ This suggests a need for a critical analysis of the uplift capacity rating systems currently in use, as well as a need for a better understanding of the load-deformation behavior of standing seam metal roof systems, and the transfer of load to the roof clips where failure usually initiates in high wind events.

Additionally, fundamental studies are required of the load distribution among roof clips at failure due to wind uplift pressures. Due to the non-uniformity of actual roof loads, experimental failure mechanisms observed during uniform static pressure tests may not occur in practice or they may occur at different locations or different pressures. If the critical relationships or behaviors are not known, the prediction of roof capacity, which is usually controlled by the roof clips, would be difficult to determine.

OBJECTIVES OF TEST PROGRAM

This paper focuses on the wind uplift performance of standing seam metal roofs. An exploratory investigation was carried out to develop a method of reproducing the effect of fluctuating roof loads on a clip using an equivalent uniform pressure apparatus. The goal of this research project, sponsored by the Metal Building Manufacturers Association (MBMA) and the American Iron and Steel Institute (AISI), is to establish the foundation for an improved uplift pressure test for standing seam metal roofs. To accomplish this task, three lines of investigation were pursued:

- Establishment of the uplift capacity of a roof specimen, using the load-deflection and failure modes obtained in the ASTM E 1592-94 test method.⁴
- Investigation, using influence surfaces, of the uplift load transferred from a standing seam metal roof specimen to the interior roof clip fasteners, and the load distribution among them.
- Development of a technique for simulating dynamic wind load effects on a roof clip using a uniform pressure test apparatus.

Through this series of experiments, baseline test results were established using the ASTM E 1592-94 procedure for standing seam metal roof systems, and the effects of various test specimen end-restraints on roof clip loads were determined. The variation of uplift loads on the interior

roof clips was also monitored to provide information on the changes in load distribution that occurred with increasing chamber pressures.

The influence surfaces for uplift loading on the roof clips were determined at four static pressure steps. In this way, a more realistic estimate of the uplift loads transferred from roof panels to the roof clips could be obtained. An estimate of the upward clip load could be determined by integrating the many individual spatial roof loads gathered through a wind tunnel study on a model building, with their respective influence coefficients for a roof clip fastener. Structural behavior was observed for two roof specimens subjected to such an equivalent uniform hurricane load time-history. This load trace was developed by Ho, Surry and Davenport of the University of Western Ontario (UWO), using wind tunnel pressure data and this set of experimentally determined influence coefficients.

BEHAVIOR OF STANDING SEAM METAL ROOFS

Standing seam metal roofs typically consist of steel or aluminum roof panels 12 inches to 30 inches (300 mm to 762 mm) wide, joined at their sides by standing seams (ribs). These seams lend structural support to the system while providing a secure connection between adjacent panels. The seams can also form a watertight seal, "standing" above the roof runoff waterline.

Roof clips are installed along the seams and are typically spaced at 2 ft. 6 in. or 5 ft. (0.76 m or 1.52 m) on centers. These roof clips, which are fastened to the supporting roof purlins or nailers, are designed to allow thermal movement along the length of the seams. Using a seaming tool, the seams along adjacent panels are rolled and seamed together as shown in Figure 1, or, with some panel designs, the seams are simply snapped together.



Figure 1. Rolled seam over purlin showing clip fastener.

Under upward pressure, the flexible flat "pans" of standing seam roof panels assume the shape of a semi-cylindrical stiffened shell spanning between the seams. A small uplift pressure of around 5 psf (0.24 kPa) is sufficient for this deformation to occur. The maximum displacement usually occurs along a panel centerline, midway between two supporting purlins/nailers. The deformed roof panel profiles shown in Figure 2 were observed during the course of the experiments. As the upward pressure is increased, the

panel displacement increases, eventually reaching a maximum deformation of 8 inches to 10 inches (200 mm to 250 mm), at or near to the failure load of the roof clips.

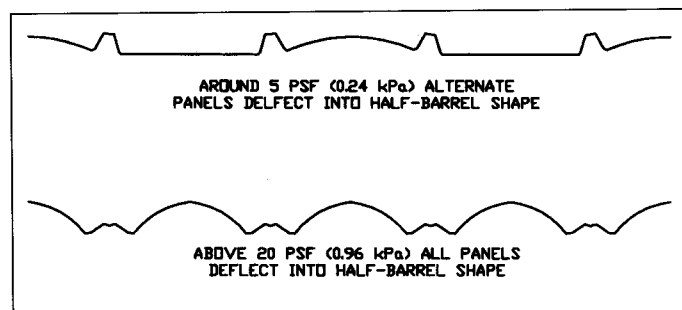


Figure 2. Configurations of deformed roof panels.

Failure of standing seam metal roofs due to uplift pressures are initiated mainly in two ways: rotation and spreading of the seams caused by panel deformation that allows the clips to slip out from the panels; and fracture of the roof fastener components. In this test series, both failure modes were observed, with the former one being the more common mode. In practice, standing seam roof systems have also been observed to fail by tearing of the roof panels themselves. This failure mode is probably initiated by high winds blowing over a roof, lifting up and tearing the roof panels. However, such effects could not be simulated using these test procedures.

TEST SETUP

All tests were conducted using 25 ft. 6 in. (7.77 m) long standing seam metal panels from one manufacturer. The 24-gauge (0.61 mm) steel panels were 24 inches (610 mm) wide with 3-inch (75 mm) high trapezoidal ribs, with two minor longitudinal stiffening ribs along the third points of the pan. The trapezoidal edge-ribs provided an installation tolerance for fastener placement, as well as permitted thermal expansion and contraction movements perpendicular to the seams. A 26 ft. long x 13 ft. wide x 15 in. deep (7.9 m x 4.0 m x 0.375 m) pressure chamber was built at Clemson University's Wind Load Test Facility for this experiment. The chamber dimensions were chosen based on the minimum specimen size specified by the ASTM E 1592-94 in an attempt to minimize the boundary effects on panel deflection results. The roof panels were connected to 8-inch (200 mm) deep Z-purlins bolted to the chamber side walls. The Z-purlins were spaced at 5 ft. (1.52 m) for all tests. Care was taken to ensure that recommended installation procedures were followed during the construction of each specimen.

Five full-width sheets and two narrower off-cuts, 18 inches (450 mm) wide were necessary to cover the chamber. As discussed in ASTM E 1592-94, a 25 ft. 6 in. (7.8 m) long, 3 in. x 3 in. x $\frac{5}{16}$ in. (75 mm x 75 mm x 8 mm) mild steel angle was attached to each off-cut panel edge parallel to the seams to prevent buckling of the flats. Each sheet was installed individually and seamed to the next one. A plan view of the pressure chamber and standing seam roof specimen is shown in Figure 3. The test arrangement facilitated the installation of specimens with various boundary conditions (i.e., it was possible to individually restrain the pans at either panel end, and/or the long panel edges parallel to



Figure 3. Chamber with attached standing seam metal roof specimen under uplift pressure.

the seams). Thus, separate experiments could be done to monitor the clip fastener load distributions on interior roof areas, edge or gable areas, and corner regions of a roof.

BRERWULF

The BRERWULF (Building Research Establishment Real-Time Wind Uniform Load Follower) system was used to apply uniform pressure to the samples. This apparatus was designed to simulate the effect of wind loads on building cladding. The bipolar valve, mounted to the test chamber, diverts airflow from a high volume low pressure fan unit into and out of the test chamber, thereby creating either positive or negative pressures inside the chamber. Because the pressure inside the test chamber is essentially uniform, it is not possible to duplicate the spatial variation of loading that actually occurs during a windstorm. However, by using a computer feedback system, the bipolar valve can be programmed to apply a pre-defined time varying pressure load trace to a specimen.

Measurement and Instrumentation

Twelve of the 30 roof clips were instrumented with custom load cells to measure the vertical load in the fasteners connecting each roof clip and the Z-purlins. The instrumented clips had nominal tributary areas of 10 sq. ft. (0.93 m²), and were located at the four interior clip positions of the purlins marked "LEFT," "CENTER" and "RIGHT" on Figure 4. In addition, a standard 1000-lb. (4.45 kN) capacity load cell was used in series with a 100-lb. (0.44 kN) spring scale during the influence surface determination to monitor the applied concentrated load.

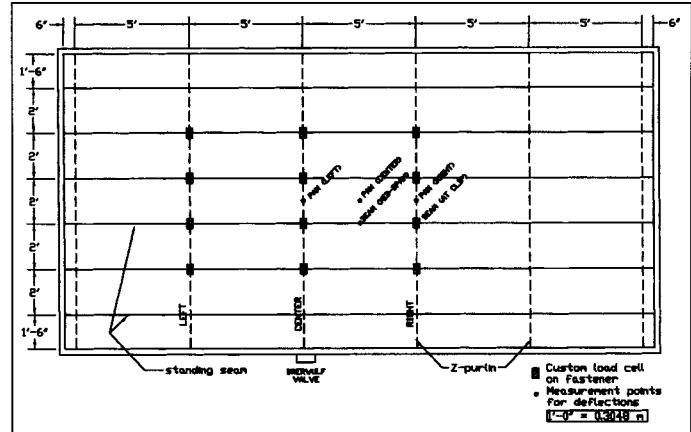


Figure 4. Location of the instrumented clip fasteners and deflection measurements.

A custom load cell and its typical attachment are shown in Figure 5. The output voltage from the load cells and BRERWULF transducers were input into a computer data acquisition package DT VEE[®] for subsequent analysis. The roof fastener load cells had to be loosely attached to the Z-purlins in order to maintain zero reading, as any pre-tensioning of the clip bolt would produce measuring errors at lower loads.



Figure 5. Custom load cell attached to failed fastening clip.

Panel deflections were monitored at five points; three points along the center of the middle flat pans, and two along the standing seam itself as shown in Figure 4. Cables attached to these points were used to monitor the panel movement and the displacements were observed on a vertical scale.

STANDARD TESTING PROCEDURES FOR METAL ROOFS

While there exist no universally recognized test procedures for metal roofing panels in the United States, individual organizations have developed separate test methods that are presently in use. The three most common tests used for metal roof panel systems are: the Factory Mutual (FM) 4471,⁶ the Underwriters' Laboratory (UL) 580,⁷ and the American Society for Testing and Materials (ASTM) E 1592-94.⁴ Each of these test methods attempts to relate its test results to critical in-field performance. However, because the stated failure criteria differ among the three methods, it is difficult to relate the results to one another or to a general performance standard. In addition, all three test methods are silent on the actual definition of an acceptable level of roof performance. It may be stated that the failure occurring during a test may be beyond the practical "performance" failure level of the roof system. However, standard tests do provide the basis for assessing the relative performance of different types of roof systems. At the suggestion of the MBMA, the ASTM method was selected as the baseline test for this investigation.

Standard ASTM Procedure

The ASTM E 1592-94 test procedure that was followed is fully described in Reference 4, and therefore an extensive account will not be repeated here. It is used to evaluate the structural performance of sheet metal panels and clips under uniform static air pressure differences. The loading cycle is begun by applying a reference-zero pressure of 5 psf (0.24 kPa) for one minute to the roof specimen, then increasing the pressure to one-third the expected failure load and holding for another minute. The chamber pressure is returned to reference between each step and held for one minute. At each step and again at the reference pressure, panel deflection measurements are taken. Each pressure step is approximately one-sixth the expected failure load higher than the previous one, and the chamber pressure is increased in this manner until failure occurs or until the roof panels can no longer maintain steady chamber pressure. Results of the ASTM test are the load-deflection curves from which the yield and ultimate strengths of the roof system are determined. A typical pressure time-history used for the ASTM test and resulting clip fastener load variations are shown in Figure 6.

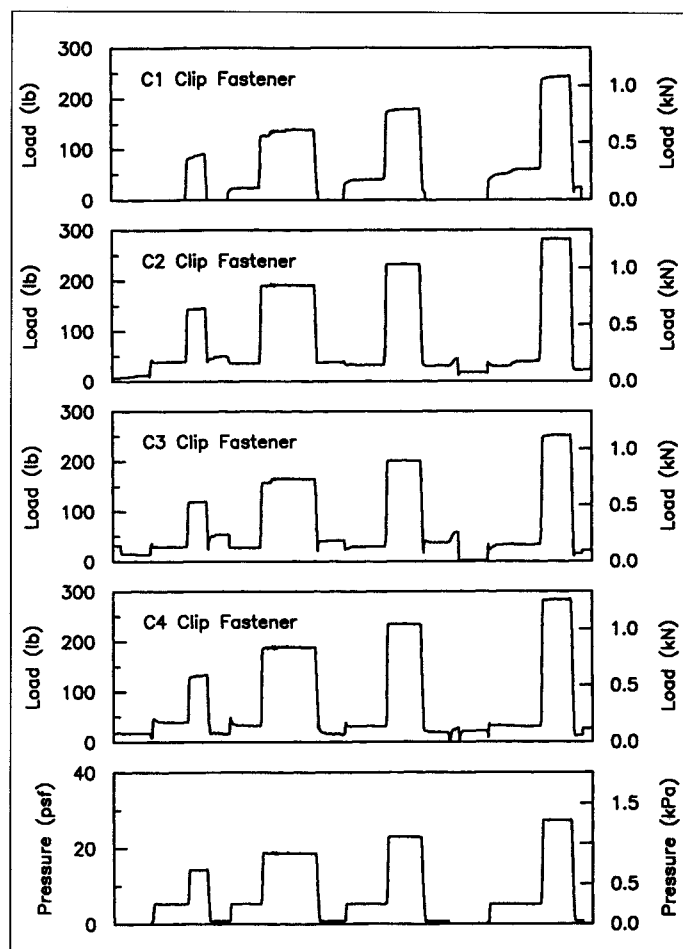


Figure 6. ASTM E 1592-94 loading and responses of clip fasteners on center purlin.

ASTM Experiments

A total of six tests were performed in accordance with ASTM E 1592-94. In two of them, the flat pan ends between the standing seams were fixed (using screws) to the extreme Z-purlins in the chamber. Two tests were done on samples having unrestricted pan ends. One test was performed on a specimen with one end fixed and the opposite end free. A final test was done on a pre-loaded (prior dynamically loaded) specimen that also had both ends free.

From the load-deflection graph in Figure 7, it is observed that large deformations of the roof system begin at approximately 25 to 30 psf (1.2 to 1.4 kPa). The ultimate load capacity could not be firmly established, but at approximately 50 psf (2.4 kPa), most samples were incapable of holding the static pressure for the required time of one minute because of excessive air leakage due to deformed seams.

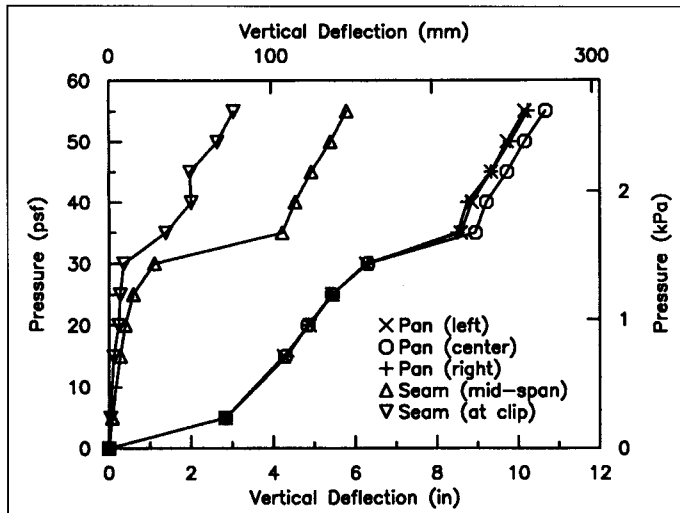


Figure 7. Load-deflection relationship for a roof specimen subjected to ASTM E 1592-94 loading.

As expected, the samples with ends clamped produced the smallest vertical deflection, and the samples with both ends free, the largest. It was also observed that only in the latter case did the deflections appear nearly constant along the panel centerline. With both ends clamped, a maximum deflection occurs around the chamber midpoint, while the sample having one clamped edge produced a sloping panel profile pointing towards the clamped edge. Another observation was that the clamping of panel ends produced premature buckling in the seams and dimpling in the flat pans occurred at relatively low pressures, 15 to 20 psf (0.72 to 0.96 kPa). In all cases these premature deformations were permanent and severe enough to limit the panels' ability to return to the unloaded profile. The specimens with free edges showed no panel buckling as in the previous cases.

The premature buckling of the seams was most severe when both ends were clamped. Other end conditions were investigated because it is uncommon in current construction practice for both panel ends to be clamped as this would restrict thermal movement. When only one end was fixed in place, the deformations were less severe, but as shown by the flat transition zone in Figure 8, the stiffened-shell sheet profile is distorted by the effect of load sharing that is taking place between the roof panels' end-fixing screws and the adjacent row of roof clips. Thus, it appears that even with this relatively large pressure chamber size, the clip loads can still be affected by the boundary conditions, although the panel deflections measured in the middle may be the same in both the restrained-end and unrestrained-end cases.

Another useful feature of the ASTM test is the measurement of the permanent set of the panels, which is defined as the deflection after a particular load value is reached and then the pressure is reduced to the reference pressure. These results, shown in Figure 9, clearly show when yielding of the material has occurred. The large permanent displacements observed after the 30 psf (1.4 kPa) and 35 psf (1.7 kPa) loads are indicative that yielding of some system components had taken place. It is difficult to determine which component has actually yielded since the measured deformation accounts for the total vertical movement, which can comprise deflections of the supporting Z-purlins, clips and clip fasteners, as well as roof panel movement.

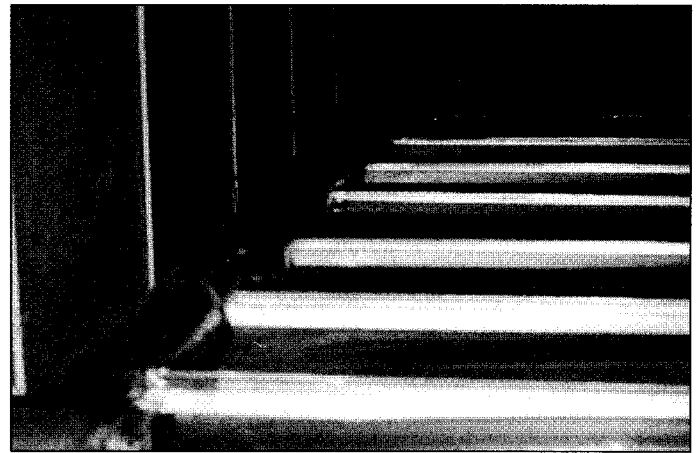


Figure 8. Deformed specimen with fixed pan end condition.

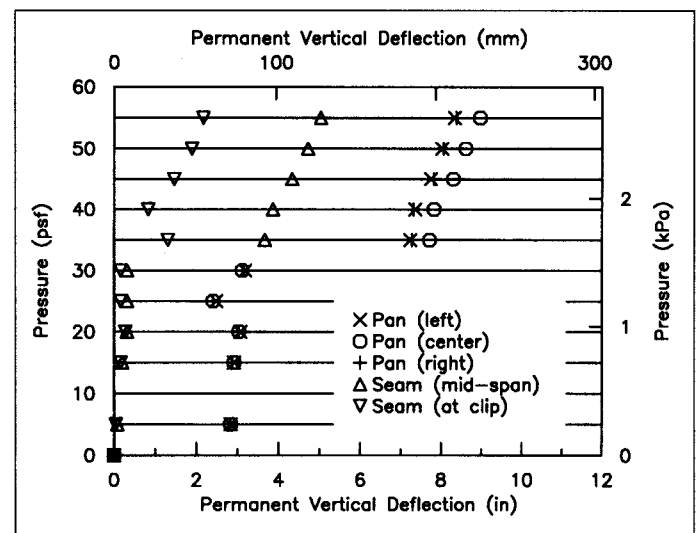


Figure 9. Permanent deformation after each pressure cycle.

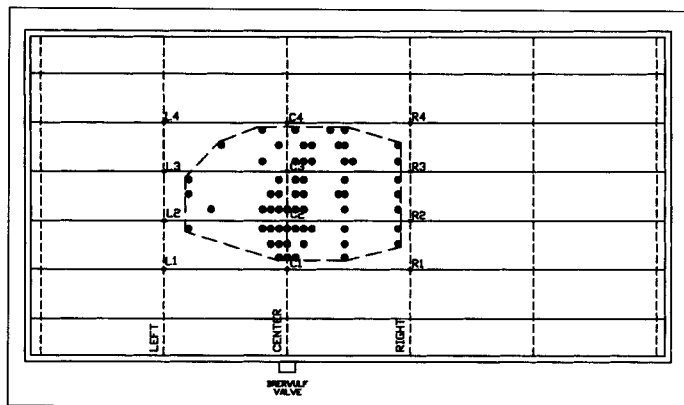
INFLUENCE SURFACE EXPERIMENT

As implied earlier, all roof and wall surfaces experience the random spatial and temporal variations of external wind loads. Therefore, the estimation of wind loads based on a uniform pressure over a particular tributary area is a conservative method that is in current use today. One drawback of this approach is that the noncorrelated peaks and valleys produce a large scatter pattern and therefore an equivalent uniform load bearing only slight resemblance to the applied one. Since it is known that wind loads are much better correlated over smaller areas, approximately 1 sq. ft. (0.09 m²), a better estimate of the true roof load may be obtained if the loads on such incremental areas are added together. Influence lines and surface approach provides a method by which this could be done, as well as accounting for variations of loads with time.

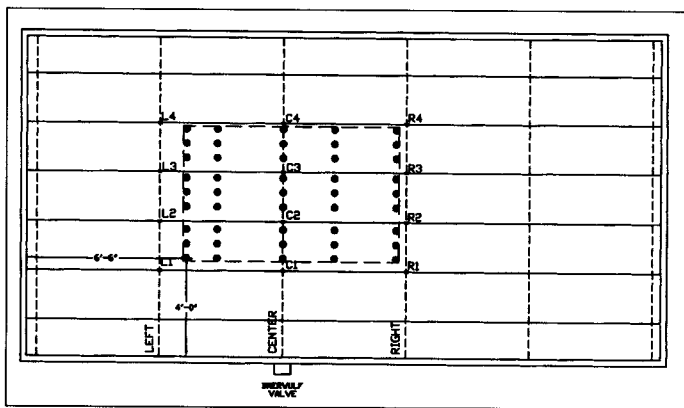
The influence surface experiment was conducted for the uplift pressure on standing seam roof clips, using a fixed point load of 100 lbs. (0.44 kN) applied at a series of grid points on the roof panels. By measuring the fastener load produced by this single point load at a series of locations on the roof, it was possible to determine the relative effects of position of an applied load, and the load transfer from each

position can be related back to the applied load. The two arrays used in this experiment are shown in Figures 10a and 10b. Using the two grid patterns ensured that any rapid decay in influence coefficients moving away from the clip would be recorded, as well as providing coverage over a sufficiently large distance from the clip. Since identical results were obtained using both grid arrangements, only the results from the larger, more uniform grid are reported.

Figure 10. Location of grid points for influence surface determination.



(a) Grid points concentrated around C2 and C3 clips.



(b) Evenly distributed grid points.

The loads transferred to six interior roof clips were simultaneously recorded, and these values were used to compute their influence surfaces. The coordinates of each grid point along with the load transfer from that location to each respective clip was the input data for the contouring software package FASTTABS,⁸ which generated the influence surfaces.

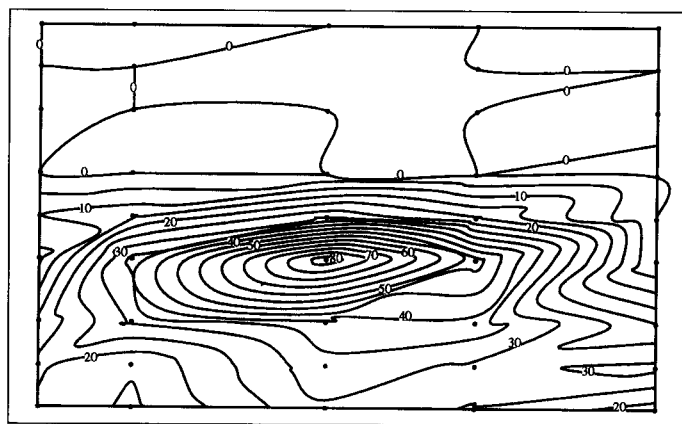
Initially the influence surfaces were generated for the unloaded zero base (or atmospheric) pressure case. The influence surfaces obtained for the clips at C2 and C3 on the center Z-purlin had similar shapes. Although only one-half of the influence surfaces were generated for the clips on the left and right Z-purlins, similar patterns were also observed. The results suggest that an asymmetry in the influence surface exists for uplift load on the clips. This may be explained by the clip construction which is eccentrically loaded in the first place.

The influence surface test was repeated with the base pressures set at 5 psf (0.24 kPa), 10 psf (0.48 kPa) and 20 psf (0.96 kPa), respectively, because the roof panel profile

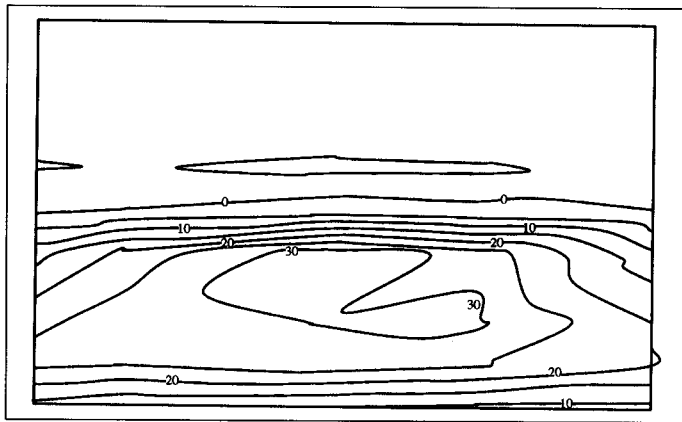
changes so much when it is under pressure. It was believed that the influence surface from the displaced roof profile would provide the data necessary to quantify any effect the changing panel geometry has on load-transfer mechanisms.

The influence surfaces for the C2 clip taken at 0 psf (0 kPa), 10 psf (0.48 kPa) and 20 psf (0.96 kPa) are shown in Figures 11a through 11c. In the zero base pressure case, most of the load transfer comes from the closest grid points around the clip, represented by an oval footprint extending 6 feet (1.82 m) longitudinally and 16 inches (0.4 m) transversely away from the clip. Within this footprint, the percentage load transferred to the clip from each grid point, $([\text{fastener load} \div \text{applied load}] \cdot 100 \text{ percent})$, ranges between 40 and 80 percent of the load applied at the grid point. The remaining load is shared among adjacent fasteners.

Figure 11. Influence surfaces for clip fasteners at C2 location.



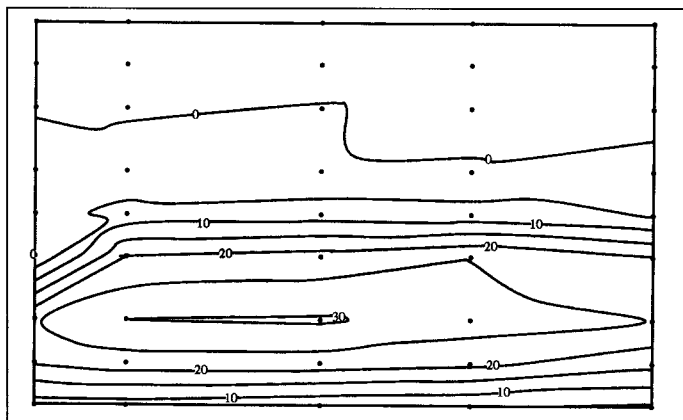
(a) Base pressure: 0 psf (0 kPa).



(b) Base pressure: 10 psf (0.48 kPa).

For the 10 psf (0.48 kPa) as well as the 20 psf (0.96 kPa) base pressure cases, the maximum load transferred from any point fell to about 60 percent and 30 percent, respectively, of the applied load. The load transfer area for the 20 psf (0.96 kPa) case (25 to 30 percent) extends 7 feet (2.14 m) longitudinally and 10 inches to 12 inches (0.25 to 0.3 m) transversely away from the C2 clip. Thus, it can be seen that with a stiffer panel configuration that a larger percentage of applied load is spread away from particular fasteners.

While the peak load transfer has been lowered for the higher base pressure case, the area of influence from which 20 percent or more load is transferred back to the fastener



(c) Base pressure: 20 psf (0.96 kPa).

has increased, especially in the longitudinal direction. It is also interesting to note that the majority of the load transfer comes from the two panels directly connected to the clip. This is in contrast to the theoretical influence surfaces utilized by Ho, Surry and Davenport.² In their paper, a continuous beam analogy was assumed, but it now appears that there is little transverse continuity away from the clip, while longitudinally the clip load comprises the load effect from at least a complete purlin span away. Some doubts remain, however, due to the inadequacy of the load cell arrangement to measure vertically downward loads.

HURRICANE TIME-HISTORY LOADING

The reason for developing the influence surfaces for uplift clip loads was to determine whether an equivalent uniform pressure apparatus such as BRERWULF, could be used to apply a representative hurricane time-history of loading to specific roof clips. The time-histories of wind speed and direction were determined by a hurricane simulation program developed at the University of Western Ontario (UWO) Boundary Layer Wind Tunnel Laboratory. This companion study simulated the most severe five-hour period of Hurricane Andrew's passage over Dade County, Florida.

Using a 1:50 scale model of a 100 ft. x 150 ft. x 16 ft. high building (30.5 m x 45.8 m x 4.88 m), with a gable roof sloping at $\frac{1}{4}$ in 12 (2 percent), personnel at the University of Western Ontario obtained wind tunnel data⁹ from a 12 ft. x 25 ft. (3.66 m x 7.62 m) interior roof panel. This data was then used to determine the effective uniform pressure time-histories using the Clemson-derived influence surfaces. An interior panel was chosen to be consistent with the boundary conditions that were simulated experimentally.

Using a 128-channel solid state scanner system, time-histories of pressures at all pressure taps placed within the dashed line around the C2 and C3 locations, shown on Figure 10(b), were simultaneously recorded. The UWO study followed the wind speed and direction of Hurricane Andrew, choosing the range of angles so that the maximum storm speed coincided with the worst direction aerodynamically for the interior roof area of the building. The time-histories of wind loading were determined by integrating the Hurricane Andrew wind pressure, aerodynamic data from the wind tunnel and the influence coefficients. In equation form, the UWO calculations can be expressed as follows:

$$L(\alpha, t) = \frac{1}{2} \rho [\sqrt{(\alpha)}]^2 \sum_i [C_{pi}(\alpha, t) \beta_i A_i] \quad (1)$$

where:

- $L(\alpha, t)$ = Total load at time t , for wind direction α
- $\sqrt{(\alpha)}^2$ = Dynamic pressure due to wind velocity $\sqrt{}$, at reference height
- (α, t) = Pressure coefficient at the i^{th} location
- β_i = Structural influence coefficient at the i^{th} location
- A_i = Tributary area at the i^{th} location

The maximum peak suction pressure measured at any location, for this interior panel, was -30 psf (-1.44 kPa), and this value was cut almost in half to -17 psf (-0.81 kPa), after averaging all pressure values over the influence area. This spatially averaged wind pressure is much lower because the pressures due to external fluctuating winds are poorly correlated with respect to one another.

The maximum frequency response of the full-size panel was on the order of 0.5 Hz. The time-histories of the equivalent uniform pressures were therefore filtered at 0.25 Hz, 0.5 Hz and 1 Hz. This filtering of the high frequency signals resulted in a further reduction in the maximum equivalent peak pressures to approximately -10 psf (-0.48 kPa).

This resulting time-history provided surprisingly low effective pressure values. Due to the interior panel location, failures would rarely be initiated there. Peak local suction near corner edges from the same wind tunnel tests and wind speed conditions would have been about -280 psf (-13.41 kPa). An interesting study would be to compute the influence functions and wind pressures for these more severely loaded roof perimeter regions. In those locations, the spatial variation of wind pressures is even more pronounced than in the field of the roof, so, although the maximum suction at any point would be high, the actual clip loads may still not reach very high values. It must be remembered that these calculations have neglected the potentially significant internal pressures that may be caused by breaching the building envelope on the windward wall. As internal pressures are more closely correlated spatially than the external pressures,¹⁰ the static pressure test may be a better indicator of panel failure initiated by internal pressure.

A five-hour dynamic trace was run on two roof specimens using two filtering frequencies of 1 Hz and 0.5 Hz. After the tests, both samples were capable of maintaining static pressure and showed no significant distress. In the second test, two load cells came loose because the fasteners attaching them to the purlins had worked free or fractured. However, these failures were attributed to the test setup rather than any overloading condition, since these fasteners were purposely left loosely attached, to obtain repeatable zero readings. After that test was completed and having replaced the fractured fasteners, a test per ASTM E 1592-94 was performed on the sample. The results showed that larger initial deflections occurred than in previous tests, but otherwise the load-deflection curves were similar to those previously obtained.

CONCLUSIONS

The load-deformation behavior of a standing seam metal roof is highly non-linear, and it has been shown that a small

upward pressure causes large deformations in the roof profile. Since distinct influence surfaces were obtained at different base pressures, it has been established that the geometric non-linearity of the panels significantly affects the load transfer mechanisms. As the failure of roof clips are determined in large measure by the upward loads in them, to predict the roof panel failure loads it is necessary to understand how this load is transferred from the roof panels to the clips. The approach presented in this paper, based upon the use of influence surfaces, may provide a better idea of the spatial variation in load transfer mechanisms and provide a reasonable estimate of the actual roof clip loads.

If it is assumed that each influence surface is valid over a range of pressures, then by selecting the appropriate influence surface to develop an equivalent uniform pressure time-history, the dynamic performance of a roof component can be investigated at ultimate load capacity or at any other load/limit state falling within the specified pressure range. Therefore the ultimate capacity of a roof component can be determined using a uniform pressure test apparatus, if there exists a stable roof geometric configuration at ultimate load for which an influence surface can be found. The likelihood that this is the case is increased due to the fact that the well-correlated internal pressure effects may dominate the overall roof loads at the ultimate capacity.

From observations of clip fastener loads during the tests, it has been determined that the choice of specimen end restraints can significantly affect the clip fastener loads, even with a chamber of this size. Therefore, the test results should be carefully interpreted before applying them to any roof arrangement. A roof specimen that is restrained at its ends sustains permanent deformations/damage at lower pressures than would a roof specimen with no end restraints. Since this premature damage may or may not affect the ultimate roof specimen failure capacity, these results suggest that an additional service performance level should be established through standard test procedures.

An investigation of a procedure that uses equivalent uniform pressures to reproduce the effect of the fluctuating roof loads on a specific roof component was performed. The method requires that influence surfaces be first determined. The procedure was demonstrated using an equivalent uniform load time-history for a five-hour hurricane and influence surfaces for an interior roof clip.

This investigation has also shown that the influence surfaces for uplift clip fastener loads on standing seam metal roof clips can extend longitudinally more than 4 feet (1.21 m) away from the clip, and therefore future influence surface experiments should extend over a larger area than was used here. Provision should also be made to measure the negative (or downward) loads, if any, that may be transferred to the roof clip. Assuming that the influence surface can be determined for other structural effects, this method is suitable for estimating the uniform loads that would produce component loads and stresses equivalent to those produced by the true spatially-varying wind loads on a building.

ACKNOWLEDGMENTS

The authors wish to acknowledge the financial support of the Metal Building Manufacturers Association, the American Iron

and Steel Institute, the Federal Emergency Management Association, the State of South Carolina and the Department of Civil Engineering at Clemson University.

The authors also would like to express sincere thanks to the following students from Clemson University: Ryan Wright, Bala Sockalingam, Tom Reed, Ed Sutt Jr., Blair Garcia, Kevin Shoemake and Nathan Nabors, for their dedicated assistance in fabricating and testing the roof specimens, and to Jeff Morin and Brice Urquhart for their help with fabricating the load cells.

REFERENCES

1. Smith, D.A., Mehta, K.C., Yeatts, B.B. and Bhavarju, S.V., "Area-averaged and internal pressure coefficients measured in the field," *Journal of Wind Eng. Ind. Aerodynamics*, Vol. 53, 1994.
2. Ho, T.C.E., Davenport, A.G. and Surry, D., "Characteristic Pressure Distribution Shapes and Load Repetitions for the Wind Loading of Low Building Roof Panels," 1994, Boundary Layer Wind Tunnel Laboratory, London, Canada.
3. Smith, Thomas L., "Insights on metal roof performance in high wind regions," *Professional Roofing*, Feb. 1995.
4. American Society of Testing and Materials, "Standard Test Method for Structural Performance of Sheet Metal Roof and Siding Systems by Uniform Static Air Pressure Difference," E 1592-94, May 1994.
5. Data Translation, Inc., *DT VEE Reference Manual*, Nov. 1993, Marlboro, Mass.
6. Factory Mutual Research, Approval Standard for Class 1 Metal Panel Roofs," Rev. VIII Class Number 4471, May 1994, Norwood, Mass.
7. Underwriters Laboratory, Inc., "Standard for Safety Tests for Uplift Resistance of Roof Assemblies," Dec. 1989, 3rd edition, Northbrook, Ill.
8. Engineering Computer Graphics Laboratory, Brigham Young University, *FASTABS- Hydrodynamic Modeling Reference Manual*, 1994, Brigham Young University, Provo, Utah.
9. Ho, T.C.E., Personal communication, May 1995, London, Canada.
10. Holmes, J.D., "Wind pressures on tropical housing," *Journal of Wind Eng. Ind. Aerodynamics*, Vol. 53, 1994.